Evaluation of the Heating Effect in Neutral Beam Injection Experiments of the GAMMA 10 Tandem Mirror

Hiroki OZAWA, Yousuke NAKASHIMA, Ryou YONENAGA, Katsuhiro HOSOI, Takashi ISHII, Hisato TAKEDA, Kazuo OKAWA and Tsuyoshi IMAI

Plasma Research Center, University of Tsukuba, 1-1-1 Tennoudai, Tsukuba, Ibaraki 305-8577, Japan

(Received 7 December 2009 / Accepted 7 May 2010)

Neutral beam injection heating has been studied for high-density mode plasma in the GAMMA 10 tandem mirror. During NBI heating, the increase in diamagnetism was found to be larger for the high-density mode plasma than the hot-ion mode plasma. A numerical model using zero-dimensional particles and energy balance equations was developed to investigate NBI heating in the central cell area. The evolution of total energy density was found to be consistent with that of diamagnetism in the low-density hot-ion mode. The initial ion temperature is a key parameter for enhancing beam heating. In high-density mode, discrepancies were found between the measured diamagnetism and the calculated total energy density. It is probably because that time behavior of the electron temperature is not suitable.

Keywords: NBI, GAMMA 10, tandem mirror, hot-ion mode, high-density mode

DOI: 10.1585/pfr.5.S2084

1. Introduction

Neutral beam injection (NBI) is one useful method for plasma heating in magnetic confinement plasma devices. It has been widely used in open magnetic confinement systems as well as toroidal confinement systems, such as tokamak and helical devices [1–4].

GAMMA 10 is a minimum-B anchored tandem mirror device with thermal barriers at both ends as shown in Fig. 1 [5]. The central cell is a simple axisymmetric mirror whose length is 6 m. The plasma is initiated by plasma guns at the both ends, and is sustained by ion cyclotron range of frequency (ICRF) heating waves. In GAMMA 10, neutral beam injectors (NBI) have been installed at the plug/barrier, anchor and the central regions. The central-cell NBI (NBI-c) system is used for main plasma heating and particle fueling. The plasma density is significantly increased by the NBI-c and the anchor NBI [3].

There are two operation modes in GAMMA 10. One is the hot-ion mode in which strong ICRF heating of the low-ion-density plasma is used to produce high ion temperatures [6]. However, the NBI heating effect is low in hot-ion mode plasmas. Recently, NBI experiments were carried out in high-density mode plasmas with strong gas puffing, since it was anticipated that the total energy density in the central cell region would be enhanced by strong beam absorption. The objective of this study is to compare the heating effects of NBI between hot-ion mode plasma and high-density mode plasma. In section 2, the experimental setup and results for the two types of plasmas are described. In section 3, the numerical simulations carried out in this study are described. Finally, in section 4, the heating results are discussed and a comparison made between the two operation modes.

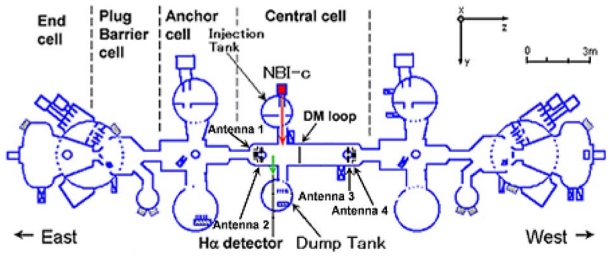

Fig. 1 Schematic illustration of the GAMMA 10 tandem mirror device and the location of the central-cell NBI (NBI-c).

2. Experimental Setup and Results

A neutral hydrogen beam at 25 keV and 30 A is injected perpendicularly at a position 123 cm away from the mid-plane of the central cell. The maximum beam duration of the injector is 100 ms. An array of five Hα detectors is installed along the machine axis (z-axis). Each detector consists of a Hα interference filter, optical fiber, lens and photo-multiplier with a magnetic shield. A microwave interferometer to measure the electron line-density (NL_{cc}) is located near the mid-plane of the central cell. Diamagnetic loops to measure the diamagnetism of the central cell (DM_{cc}) are also installed in the central cell. DM_{cc} is proportional to the stored energy of the central-cell plasmas. The data obtained from the loop nearest to the mid-plane are used in this study.

The main plasma in the central cell is generated using

author's e-mail: ozawa_hiroki@prc.tsukuba.ac.jp

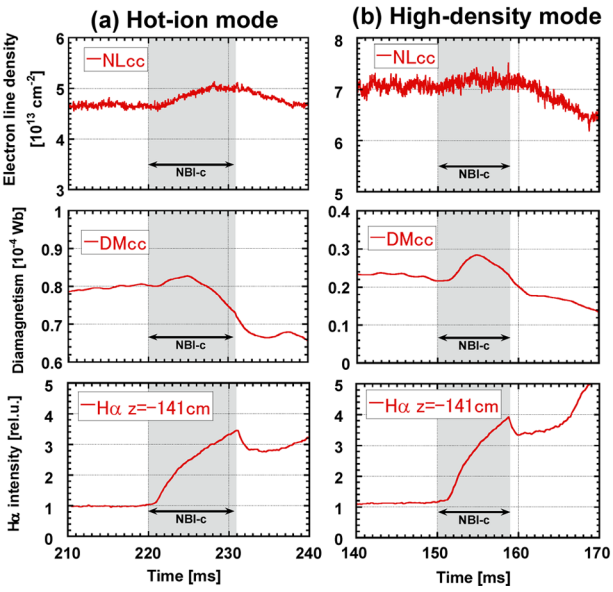

Fig. 2 Temporal behavior of plasma parameters in the central-cell NBI experiment. (a) results for hot-ion mode. (b) results for high-density mode. Top figures are electron line density (NL_{cc}). Middle figures are diamagnetism (DM_{cc}). Bottom figures are Hα intensity at z = −141 cm.

ion cyclotron heating and gas puffing. One of the ICRF waves (RF1: 9.9 MHz) is used for MHD stabilization of the entire plasma at the anchor cell. Another wave (RF2: 6.3 MHz) is used for heating the central-cell ions by ion cyclotron resonance near the mid-plane of the central cell. Four antennas (Antenna 1-4) for ICRF waves are used in GAMMA 10; two are installed near each end of the central cell. In hot-ion mode, RF1 waves are excited by Antenna 1 and 4 and the other antennas are used for RF2. The ion temperature achieved in the central cell is about 3-5 keV. NL_{cc} is about $3\text{-}5 \times 10^{13}$ cm^{-2} in this operation mode [6]. On the other hand, in high-density mode, RF1 is excited by Antenna 1, 3 and 4 and Antenna 2 is used only for RF2. Although the plasma density is comparatively higher than that of hot-ion mode, the ion temperature is less than 1 keV. Seven gas puffers are installed in the central cell and most are located away from the resonance layer of the ICRF wave in order to avoid charge-exchange loss of hot ions.

Figure 2 (a) shows the time behavior of NL_{cc}, DM_{cc} and Hα line-emission in the NBI experiment carried out in a typical hot-ion mode plasma. Shaded areas represent the timing of NBI-c. A beam of about 20 keV and about 20 A is injected. NL_{cc} is observed to increase by approximately 10% during the NBI pulse in hot-ion mode. DM_{cc} also increases by several percent in the initial period of NBI, and then decreases by 10% or more in the course of the NBI pulse. It is thought that this reduction occurs as a result of plasma cooling due to an increase in the charge-exchange reaction because of enhanced hydrogen recycling and cold gas influx induced by NBI. A sharp increase in the Hα intensity is observed near the injection port (z = −141 cm) for both modes, as seen in Fig. 2. This indicates a rapid increase in the neutral density caused by NBI [7].

Figure 2 (b) shows the case for the high-density mode plasma. The beam power is the same as that in the hot-ion mode. NL_{cc} is seen to increase only slightly during the NBI pulse. DM_{cc} increases initially and then decreases during the remainder of the pulse. The initial rate of increase of DM_{cc} is higher than that in the hot-ion mode plasma, and the maximum magnitude of the increase is by a factor of 1.5. It is clear that the NBI plasma heating effect in high-density mode is larger than that in hot-ion mode.

3. Modeling of the Particle and Energy Balance in the Central-Cell Plasma

In order to explain the above experiment results, a numerical simulation model was developed. The model is composed of five differential equations based on the efflux and influx of particles and energy in the central cell. The equations are spatially zero-dimensional and are solved numerically to simulate the time evolution of plasma parameters in the central cell. Similar calculation methods have been used in a study of a mirror confinement device [8]. In the simulation model reported here, the items concerned with the balance of particles and energy are subdivided. Therefore, the particle-confinement time is not treated as a free parameter but is calculated in the simulation.

The differential equations for particle balance comprise three components, describing warm ions, hot ions and neutral particles. In this model, the neutral particles around the central plasma are considered to be hydrogen atoms and are treated as cold gas with zero energy. The hot ions represent the ionized neutral beam particles. The energy of the hot ions is treated as constant and equal to the neutral beam energy. The warm ions are defined as all ions in the central cell except the hot ions. The energy balance equations consist of two components for warm ions and electrons. When considering particle balance, the electron density is assumed to be equal to the sum of the hot and warm ion density from the viewpoint of charge neutrality. These balance equations take into account ionization, charge exchange, energy relaxation time associated with coulomb collisions, mirror confinement time of the central cell and wall recycling. Each equation is shown as follows,

$$\frac{dn_w(t)}{dt} = n_0(t)[\alpha n_h(t)\{<\sigma v>_{pi} + <\sigma v>_{cx}\} + \alpha_w n_w(t)<\sigma v>_{pi} + \{\alpha_w n_w(t) + \alpha n_h(t)\}<\sigma v>_{ei}] + \frac{n_h(t)}{\tau_{sd}(t)} + S^w_{bg} - n_w(t)\frac{2r_p I(t)}{qV_p v_b}<\sigma v>_{cx} - \frac{n_w(t)}{\tau_{Mw}(t)}, \quad (1)$$

for warm-ion density n_w,

$$\frac{dn_h(t)}{dt} = \frac{2r_p I(t)}{qV_p v_b}[\{n_w(t) + n_h(t)\}\{<\sigma v>_{pi} + <\sigma v>_{ei}\} + n_w(t)<\sigma v>_{cx}] - \alpha n_0(t) n_h(t)<\sigma v>_{cx} - \frac{n_h(t)}{\tau_{sd}(t)} - \frac{n_h(t)}{\tau_{Mh}(t)}, \quad (2)$$

for hot-ion density n_h,

$$\frac{dn_0(t)}{dt} = (\gamma - 1)n_0(t)\{\delta(t)\alpha n_h(t)<\sigma v>_{cx} + \alpha_w n_w(t)<\sigma v>_{cx}\} + \delta(t)\gamma\frac{2r_p I(t)}{qV_p v_b}\{n_w(t) + n_h(t)\}<\sigma v>_{cx} + \gamma\beta\frac{I(t)}{qV_{cc}} - n_0(t)[\{\alpha n_h(t) + \alpha_w n_w(t)\}<\sigma v>_{pi} + \alpha_w\{n_w(t) + n_h(t)\}<\sigma v>_{ei}] - \frac{n_0(t)}{\tau_{pump}} + S_{is}(t) + S^n_{bg}, \quad (3)$$

for neutral-particle density n_0,

$$\frac{dW_w(t)}{dt} = Q^w_{bg} + \frac{n_h(t)\left\{E_b - \frac{3}{2}T_w(t)\right\}}{\tau_i(t)} - \alpha_w W_w(t)n_0(t)<\sigma v>_{cx} - \frac{\frac{3}{2}n_w(t)\{T_w(t) - T_e(t)\}}{\tau_e^{warm}(t)} - W_w(t)\frac{2r_p I(t)}{qV_p v_b}<\sigma v>_{cx} - \frac{W_w(t)}{\tau_E^{warm}(t)}, \quad (4)$$

for warm-ion energy density W_w, and

$$\frac{dW_e(t)}{dt} = Q^e_{bg} + \frac{m_e}{m_p + m_e}\frac{2r_p I(t)}{qV_p v_b}\{n_w(t) + n_h(t)\}\{<\sigma v>_{pi} + <\sigma v>_{ei}\}E_b + \frac{n_h(t)\{E_b - \frac{3}{2}T_e(t)\}}{\tau_e^{hot}(t)} + \frac{\frac{3}{2}n_w(t)\{T_w(t) - T_e(t)\}}{\tau_e^{warm}(t)} - \kappa\frac{W_e(t)}{\tau_E^{electron}(t)}, \quad (5)$$

for electron-energy density W_e.

Equations (1) and (2) take into account ionization, charge exchange, energy relaxation processes by Coulomb collisions and central mirror losses. $<\sigma v>_{pi}$ is the cross section for ionization due to ion collisions. $<\sigma v>_{cx}$ is the cross section associated with charge exchange between neutral particles and ions. $<\sigma v>_{ei}$ is the cross section for ionization due to collisions with electrons. α is the attenuation coefficient of neutral particles interacting with hot ions with a radial distribution. α_w is the attenuation coefficient of neutral particles interacting with warm ions. $\tau_{sd}(t)$ is the slowing time of hot ions due to coulomb collisions. S^w_{bg} is the background source and is defined to satisfy $dn_w(t)/dt = 0$ at $t = 0$. r_p is the plasma radius. $I(t)$ is the injected beam current. q is the elementary charge. V_p is the plasma volume in the central cell. v_b is the velocity of the particles in the beam. $\tau_{Mw}(t)$ is the central mirror confinement time for warm ions. $\tau_{Mh}(t)$ is the central mirror loss time for hot ions.

Equation (3) deals with ionization, charge exchange, and the pumping and wall recycling processes of neutral particles. γ is the wall recycling factor. $\delta(t)$ is the recycling delay factor. β is the ratio of beam particles hitting the walls to those shining through the central cell. τ_{pump} is the pumping time for neutral particles. $S_{is}(t)$ is the influx of neutral particles from the beam injection tank. S^n_{bg} is the background source and is defined to satisfy $dn_0(t)/dt = 0$ at $t = 0$.

Equation (4) describes charge exchange, energy relaxation due to Coulomb collisions and central mirror loss. Q^w_{bg} is the background source. It corresponds to the ICRF heating effect and is defined to satisfy $dW_w(t)/dt = 0$ at $t = 0$. E_b is the neutral beam energy. $T_w(t)$ is the warm ion temperature. $\tau_i(t)$ is the energy transfer time to warm ion from hot ion. $T_e(t)$ is the electron temperature. $\tau_e^{warm}(t)$ is the energy transfer time to electron from warm ion. $\tau_E^{warm}(t)$ is the mirror confinement time of warm ion energy.

Equation (5) describes ionization, energy relaxation due to Coulomb collisions and central mirror loss. Q^e_{bg} is the background source and is defined to satisfy $dW_e(t)/dt = 0$ at $t = 0$. m_p is proton mass. m_e is electron mass. $\tau_e^{hot}(t)$ is the energy transfer time to electron from hot ion. $\tau_E^{electron}(t)$ is the central mirror confinement time of electron energy. κ is a factor included to maintain the charge neutrality of the plasma.

4. Comparison between Experiment and Simulation

Figure 3 shows the time evolution of DM_{cc} and the simulation results for total energy density in hot-ion mode. The total energy density is given by $(W_w(t) + W_e(t) + n_h(t)E_b)$, which corresponds to the stored energy of the central-cell plasma. In the simulation, the initial values are $T_w(0) = 4\,keV$, $T_e(0) = 60\,eV$, $n_w(0) = 1.5\times10^{12}\,cm^{-3}$ and $n_0(0) = 1\times10^9\,cm^{-3}$. The simulation curve undergoes an increase by several percent during the initial 5 ms and then decreases for the remainder to the NBI pulse. Thus, the simulation approximately reproduces the experimental results in hot-ion mode.

The NL_{cc} value for high-density mode plasmas is approximately 1.5 times larger than that for hot-ion mode plasmas. However, DM_{cc} in high-density mode is approximately one third that in hot-ion mode. Therefore, the major difference in plasma parameters between hot-ion mode and high-density mode is the ion temperature. Figure 4 shows the initial ion temperature dependence of the calculated energy density. In this calculation, the values of $T_e(0)$, $n_w(0)$ and $n_0(0)$ are the same as for hot-ion mode. From the figure, it can be seen that the case with the low-

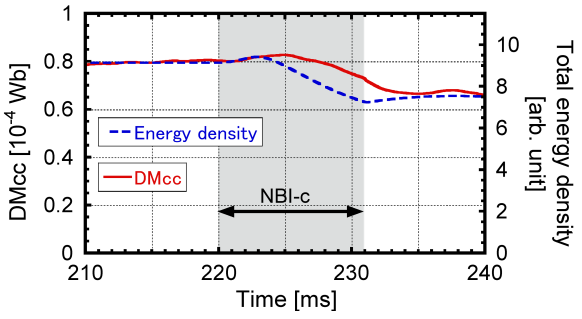

Fig. 3 Time evolution of measured DM_{cc} and simulation result of energy density in hot-ion mode plasma.

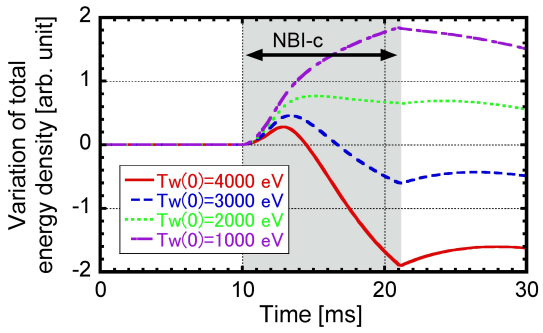

Fig. 4 Simulation results of initial ion temperature dependence of energy density during NBI pulse.

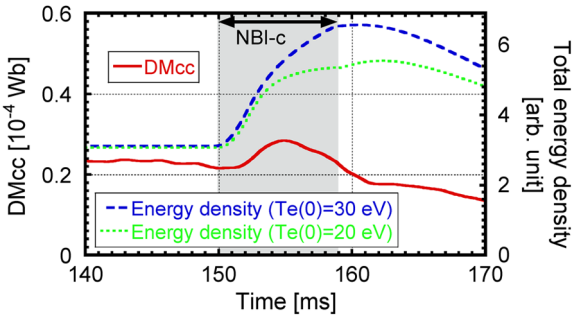

Fig. 5 Measured time evolution of DM_{cc} and simulation results of energy density in high-density mode plasma.

est initial ion temperature gives rise to the largest increase in energy density by NBI. This calculation results indicate the difference of the experimental results between hot-ion mode and high-density mode. The calculated results also show that the energy transfer rate from beam particles to the target plasma in high-density mode is higher than that in hot-ion mode. It is thought that the difference in NBI heating effects between hot-ion and high-density modes are the result of the above mechanism.

Figure 5 shows the time evolution of measured DM_{cc} in the high-density mode plasma together with the simulated energy density under similar conditions. In the simulation, the initial values are $T_w(0) = 800\,\mathrm{eV}$, $n_w(0) = 2.5\times10^{12}\,\mathrm{cm}^{-3}$ and $n_0(0) = 1\times10^{9}\,\mathrm{cm}^{-3}$ and the results are shown for two values of $T_e(0)$ (20 and 30 eV). The measured DM_{cc} increases by a factor of 1.5 in the first 5 ms of NBI and then decreases to its initial level. However, the calculated energy density increases continuously during the NBI pulse. Therefore, at present, the experimental and simulated results do not agree for the high-density mode. The ion temperature is not precisely measured in this experiment. Here, $T_w(0) = 800\,\mathrm{eV}$ is a value assumed from charge-exchange neutral particle measurements carried out in past experiments [6]. It is expected that this value has a margin of error of about 100 eV. However, from the simulations, it was confirmed that varying $T_w(0)$ in the range 600-1000 eV had no significant effect on the total energy density. As a cause of the results, the time evolution of the electron temperature might be not suitable for this experiment. Plasma confinement time is strongly affected by electron temperature in this parameter regime. At present, the electron temperature in the experiment cannot be measured accurately. As shown in the figure, the initial values $T_e(0)$ are assumed to be 20 and 30 eV. In past experiments, $T_e(0)$ of 30 eV was assumed from soft X-ray measurements. However, it appears that the simulation results with $T_e(0) = 20\,\mathrm{eV}$ are a better fit to the experimental results. In order to measure the electron temperature exactly, installation of a YAG laser Thomson scattering system at GAMMA 10 is now underway. More precise measurement of electron temperature will allow more accurate simulations to be performed.

5. Summary

Numerical calculations of plasma energy balance and particle balance were performed to clarify the difference of the NBI heating effect between hot-ion mode and high-density mode plasmas. The main difference found was in the initial ion temperature rather than the ion density. Precise estimation of the time behavior of electron temperature is needed to improve the accuracy of the calculations.

Acknowledgement

The authors would like to thank the members of the GAMMA 10 groups for their collaboration in the experiments and for helpful discussion.

[1] F. H. Coensgen *et al.*, Phys. Rev. Lett. **22**, 1503 (1975).
[2] A. Abdrashitov *et al.*, Trans. Fusion Sci. Tech. **47**, No. 1T, 27 (2005).
[3] Y. Nakashima *et al.*, Trans. Fusion Sci. Tech. **43**, No. 1T, 135 (2003).
[4] Y. Nakashima *et al.*, Trans. Fusion Sci. Tech. **47**, No. 1T, 155 (2005).
[5] M. Inutake *et al.*, Phys. Rev. Lett. **55**, 939 (1985).
[6] T. Tamano *et al.*, Phys. Plasmas **2**, 2321 (1995).
[7] Y. Nakashima *et al.*, J. Nucl. Mater. **313-316**, 553 (2003).
[8] P. A. Pincosy *et al.*, Rev. Sci. Instrum. **58**, 9 (1987).